THE JOURNAL OF BIOLOGICAL CHEMISTRY
Vol. 279, No. 28, Issue of July 9, pp. 29147–29154, 2004
Printed in U.S.A.

DNA Methylation Polymorphisms Precede Any Histological Sign of Atherosclerosis in Mice Lacking Apolipoprotein E*

Received for publication, April 1, 2004, and in revised form, May 3, 2004
Published, JBC Papers in Press, May 6, 2004, DOI 10.1074/jbc.M403618200

Gertrud Lund‡, Linda Andersson§, Massimiliano Lauria‡, Marie Lindholm§, Mario F. Fraga¶, Ana Villar-Garea¶, Esteban Ballestar¶, Manel Esteller¶, and Silvio Zaina‖**

From the ‡Institute of Plant Biology, Department of Plant Biochemistry, Royal Veterinary and Agricultural College, 1871 Frederiksberg, Denmark, §Experimental Cardiovascular Research, Department of Medicine, University of Lund, 205 02 Malmö, Sweden, the ¶Cancer Epigenetics Laboratory, Spanish National Cancer Centre, 28029 Madrid, Spain, and the ‖Department of Clinical Biochemistry, Rigshospitalet, 2100 Copenhagen, Denmark

The present work investigates the occurrence and significance of aberrant DNA methylation patterns during early stages of atherosclerosis. To this end, we asked whether the genetically atherosclerosis-prone APOE-null mice show any changes in DNA methylation patterns before the appearance of histologically detectable vascular lesion. We exploited a combination of various techniques: DNA fingerprinting, *in vitro* methyl-accepting assay, 5-methylcytosine quantitation, histone post-translational modification analysis, Southern blotting, and PCR. Our results show that alterations in DNA methylation profiles, including both hyper- and hypomethylation, were present in aortas and PBMC of 4-week-old mutant mice with no detectable atherosclerotic lesion. Sequencing and expression analysis of 60 leukocytic polymorphisms revealed that epigenetic changes involve transcribed genic sequences, as well as repeated interspersed elements. Furthermore, we showed for the first time that atherogenic lipoproteins promote global DNA hypermethylation in a human monocyte cell line. Taken together, our results unequivocally show that alterations in DNA methylation profiles are early markers of atherosclerosis in a mouse model and may play a causative role in atherogenesis.

Atherosclerosis and its complications are a major cause of death and disability in the developed world. The disease is characterized by infiltration of lipid particles in the arterial wall, accompanied by the recruitment of inflammatory and immune cells, migration and proliferation of smooth muscle cells (SMC),[1] and synthesis of extracellular matrix. These processes eventually result in the gradual development of an elevated lipid-rich, fibrocellular lesion (1).

In mammals, DNA methyltransferases use *S*-adenosyl methionine (SAM) as a methyl group donor to methylate the carbon in position 5 of cytosine residues in a CpG dinucleotide (CG) context (2). DNA methylation regulates fundamental biological phenomena such as gene expression, genome stability, mutation rate, genomic imprinting, and X chromosome inactivation (3–6). Both global and gene-specific alterations in DNA methylation are associated with abnormal phenotypes in disease (7, 8). For example, cancer cells show global genomic hypomethylation and dense hypermethylation of CpG islands, which are normally unmethylated (9). The identification of cancer type- and stage-specific changes in DNA methylation has justified hopes for novel diagnostic and therapeutic avenues (10).

Two general observations suggest that alterations in DNA methylation patterns are involved in atherogenesis (11–13). First, global hypomethylation and dense hypermethylation of certain CpG islands are associated with aging, a major risk factor for atherosclerosis (14). Second, hyperhomocysteinemia and the subsequent decreased production or bioavailability of SAM is associated with an increased risk of cardiovascular disease (15). Accordingly, mice with genetically reduced levels of methylenetetrahydrofolate reductase, a key enzyme in the pathway generating SAM, show hyperhomocysteinemia, DNA hypomethylation, and aortic lipid infiltrations (16). Furthermore, a global DNA hypomethylation has been observed in vascular lesions and leukocytes of atherosclerosis patients and proliferating SMC in animal models (17–19).

One unresolved issue is whether DNA methylation patterns are altered at early stages of atherosclerosis and are associated with susceptibility to the disease. Answers to these questions may have important implications for prevention and therapy of atherosclerosis. We therefore asked whether changes in DNA methylation patterns occur prior to the appearance of any vascular lesions in PBMC and aorta of mice lacking APOE, compared with matched WT animals (20). Moreover, in an attempt to provide a mechanism for the changes in DNA methylation patterns observed *in vivo*, we asked whether atherogenic lipoprotein profiles could affect DNA methylation and histone post-translational modifications in the human monocyte-macrophage cell line THP-1 (21). The present study is the first analysis of DNA methylation at early stages of atherosclerosis and the first description of genomic DNA sequences undergoing epigenetic changes in a mouse model. The implications of our findings for understanding human atherosclerosis are discussed.

* This work was supported by the Swedish Research Council, the Swedish Heart and Lung Foundation, the Crafoordska Stiftelsen, and Danish Research Council Grant 22-02-0578 (to S. Z.). The costs of publication of this article were defrayed in part by the payment of page charges. This article must therefore be hereby marked "*advertisement*" in accordance with 18 U.S.C. Section 1734 solely to indicate this fact.

The nucleotide sequence(s) reported in this paper has been submitted to the GenBank™/EBI Data Bank with accession number(s) AY606848–AY606871 (in the order listed in Table II).

** To whom all correspondence should be addressed. Tel.: 45-35452934; Fax: 45-35454640; E-mail: silvio.zaina@rh.dk.

[1] The abbreviations used are: SMC, smooth muscle cells; ^{m}C, 5-methylcytosine; CG, CpG dinucleotide; DMP, DNA methylation polymorphism; HPCE, high performance capillary electrophoresis; MSAP, methylation-sensitive amplified polymorphism; SAM, *S*-adenosyl methionine; PBMC, peripheral blood mononuclear cell; WDMP, wild type DNA methylation polymorphism; MDMP, mutant DNA methylation polymorphism; UK, United Kingdom; EST, expressed sequence tag; WT, wild type; LDL, low density lipoprotein; VLDL, very low density lipoprotein; HDL, high density lipoprotein; HL, high VLDL + LDL mixture; WL, low VLDL + LDL mixture.

EXPERIMENTAL PROCEDURES

Animal Work and Tissue Manipulation—All procedures used in this study were approved by the local ethical committee (Malmö/Lunds Djurförsöksetiska Nämnd, license M89-01). *Apoe* nullizygous mice (*Apoe*$^{-/-}$) of the strain created in the laboratory of N. Maeda (20) were purchased from M&B (Ry, Denmark) and were at the 10th generation of breeding on to the C57BL/6 genetic background. Four-week- and 6-month-old *Apoe*$^{-/-}$ or C57BL/6 control mice were sacrificed and dissected following overnight fasting. Dissections were performed according to anatomic maps of the mouse (22). The aortic tissue used in this study included the thoracic portion from the middle of the aortic arch and the abdominal portion to the iliac bifurcation. The initial portion of the ascending aorta was used to assess the presence of fatty lesions as described (23). PBMC were isolated by Ficoll-Paque PLUS gradient according to the instructions from the manufacturer (Amersham Biosciences, Little Chalfont, United Kingdom (UK)). Skeletal muscle tissue was dissected from the pelvic limb. Genomic DNA or total RNA were extracted by using the DNeasy or RNeasy system (Qiagen, Valencia, CA), respectively, according to manufacturer instructions. The levels of plasma cholesterol and triglycerides were measured as described (23).

Methylation-sensitive Amplified Polymorphism (MSAP) Analysis—DNA methylation profiles were analyzed by the MSAP as reported (24) with the following modifications.

Restriction Digest of Genomic DNA and Attachment of Adaptors—All enzymes used in the MSAP protocol were provided by New England Biolabs (Hertfordshire, UK). Five hundred nanograms of genomic DNA were digested for 1 h with 20 units of HpaII and EcoRI using NEB buffer 1 in a 30-μl reaction volume. Subsequently, the restriction digest and ligation reactions were carried out simultaneously for an additional 3 h in a final volume of 40 μl. The restriction-ligation mix contained 10 units of HpaII, 10 units of EcoRI, 10 units of T4 DNA ligase, 5 pmol EcoRI adaptor, 50 pmol HpaII adaptor and 1 mM ATP. The enzymes were inactivated for 15 min at 65 °C, and a second digest was performed for 1 h with 5 units of HpaII and EcoRI, again followed by heat inactivation. The adaptor sequences were as follows: EcoRI adaptor, 5′-CTCGTAGACTGCGTACC-3′ and 5′-AATTGGTACGCAGTCTAC-3; HpaII adaptor, 5′-GATCATGAGTCCTGCT-3′ and 5′-CGAGCAGGACTCATGA-3′.

Preamplification—The preamplification reaction was performed with primers complementary to the core of the adaptor sequences and the target sequence of EcoRI and HpaII restriction enzymes. The sequences of the EcoRI preselective primer (EcoRI-00) and the HpaII preselective primers (HpaII-00) were 5′-AGACTGCGTACCAATTC-3′ and 5′-TCATGAGTCCTGCTCGG-3′, respectively. Two microliters of the digestion-ligation mix (diluted 1:3) were added to the pre-amplification mix consisting of 1× PCR Buffer, 0.1 mM dNTP, 50 ng of EcoRI-00 primer, 50 ng of HpaII-00 primer, and 1 unit of *Taq* polymerase (Roche Biochemicals). The PCR conditions were as follows: 72 °C for 2 min, 94 °C for 3 min, followed by 25 cycles as follows: 95 °C for 30 s, 56 °C for 30 s, 72 °C for 1 min. A final extension was performed at 72 °C for 4 min.

Selective Amplification—The sequence of the selective primers was identical to the preselective primers but included the addition of a number of nucleotides at the 3′ terminus. The selective nucleotides of the EcoRI-00 primer were as follows: EcoRI-01, AGT; EcoRI-02, ACA; EcoRI-03, AGA; and EcoRI-04, ACC. The HpaII selective primers were: HpaII-01, TCCA; HpaII-02, TAGC; HpaII-03, CGAA; HpaII-03A, CGTT; HpaII-04, AATT; and HpaII-04A, AACC. Selective PCR was conducted using 2 μl of pre-amplification mix (diluted 1:10) in a 10-μl reaction volume containing 1× PCR Buffer, 0.1 mM dNTP, 50 ng of EcoRI-00 primer, 50 ng of ^{33}P-labeled HpaII-00 primer, and 1 unit of *Taq* polymerase. The HpaII primer was end-labeled by incubating 50 ng of primer with 50 μCi of [γ-^{33}P]dATP, 10 units of polynucleotide kinase and 5 μl of 1× OPA buffer (Amersham Biosciences, Buckinghamshire, UK). The reaction was incubated for 1 h at 37 °C, followed by heat inactivation for 15 min at 65 °C. The PCR cycle employed was a standard amplified fragment length polymorphism touchdown protocol (25).

Polyacrylamide Gel Electrophoresis—The PCR samples were mixed 1:1 (v/v) with denaturating buffer (98% formamide, 10 mM EDTA, 0.1% bromphenol blue, and 0.1% xylene cyanol) and separated on 6% polyacrylamide sequencing gel (Bio-Rad) for 3 h at 90 watts. Gels were dried and exposed to x-ray film (BioMax, Eastman Kodak Co.) for 1–4 days at −80 °C. For each experiment, two or three independent MSAP reactions, each corresponding to pooled samples from three or four mice, were performed. If the results were reproducible, one sample was used for further analysis. Quantitative analyses of band patterns were conducted on central portions of gels, where resolution was maximal.

SssI Methyl-accepting Assay—The assay was performed as previously described (26), with the exception that Nonidet P-40 was replaced with Triton and labeled DNA was blotted on a Nytran SuPerCharge membrane (Schleicher & Schuell, Dassel, Germany).

Isolation and Sequencing of MSAP Bands—Bands were excised from acrylamide gels, suspended in 30 μl of 0.5× TE buffer, and incubated for 10 min at 65 °C. One microliter of the solution was used in a standard PCR reaction with the appropriate primer combinations. The resulting fragments were cloned in the pCR®II-TOPO® vector (Invitrogen, Paisley, UK), and three independent clones were sequenced. Homology searches were conducted using NIX software (www.hgmp.mrc.ac.uk).

The CpG ratio was calculated by dividing the number of observed CG dinucleotides by their expected number, calculated with the formula (number of cytosines)(number of guanines)/(total number of nucleotides).

Southern Blotting and Methylation-sensitive PCR Analysis of DMR—Fifteen micrograms of genomic DNA were digested overnight with the appropriate restriction enzyme, blotted, and probed with selected labeled MSAP fragments. Hybridization was conducted by using the ULTRAhyb™ system according to instructions from the manufacturer (Ambion, Huntingdon, UK).

Selected fragments for which flanking sequences could be deduced from data base matches were analyzed by methylation-sensitive PCR (27). Two hundred nanograms of DNA was amplified with the following fragment-specific primers. Fragment sz44 consisted of internal primer, 5′-TAGCAGAGACCTAGAAGAGGG-3′ (forward); and flanking primer, 5′-TTCAAAAGTTGCCTCAAGTCC-3′ (reverse), corresponding to nucleotides 70314–70294 of sequence with accession no. AC103664. Fragment M54 consisted of internal primer, 5′-TGTGTTTTCCTCTCT-TAGCCC-3′ (forward); and flanking primer, 5′-TTCTCAGCCATTCGG-TATTCC-3′ (reverse), corresponding to nucleotides 86183–86163 of sequence with accession no. AC120437. Fragment M4 consisted of internal primer, 5′-AGTGCCTGTGATCCTTACCTG-3′ (forward); and flanking primer, 5′-AAAGCTCAGAGTAGAAAAGGG-3′ (reverse), corresponding to nucleotides 194754–194774 of sequence with accession no. AC132863. Conditions were as follows: 94 °C for 1 min; followed by 35 cycles at 94, 51, and 72 °C, each for 1 min; and a final extension step at 72 °C for 10 min. Predicted PCR fragments were sz44, 399 bp; M54, 327 bp; and M4, 282 bp.

Expression Analysis by Reverse Transcription-PCR—Expression analysis of leukocytic MSAP polymorphic fragments showing homology to EST or genomic sequences (see "Results") was conducted by using fragment-specific nested primers. *Gapdh* RNA was amplified as an internal control (Clontech, Palo Alto, CA). Primer identity and PCR conditions are available upon request.

Southern Blotting Analysis of LINE-1 Elements—A 548-bp probe spanning a conserved 5′ region sequence in mouse LINE-1 elements (28) was constructed by subjecting mouse tail genomic DNA to PCR with the primers 5′-ATCTTGGTTCGGGACCCGCCGAACTTAGG-3′ (forward) and 5′-GTTTACCTTTCGCCATCTGGTAATCTCTGG-3′ (reverse). Conditions were as follows: 94 °C for 1 min; followed by 35 cycles at 94, 60, and 72 °C, each for 1 min; and a final extension step at 72 °C for 10 min. The probe was sequenced and used in Southern blotting as indicated in the previous paragraph.

Cell Culture and Lipoprotein Isolation—Human THP-1 cells were maintained in RPMI 1640 medium supplemented with fetal calf serum (10%), glutamine (4 mM), penicillin (20 IU/ml), and streptomycin (20 μg/ml). Cells were either used as monocytes or differentiated to macrophages by incubation with phorbol myristate acetate (50 ng/ml) for 4 days with change of medium every second day. For experiments, both monocytes and macrophages were incubated for 24 h in serum-free media with lipoprotein additions as indicated under "Results." Lipoproteins were prepared by differential ultracentrifugation of fresh plasma from healthy donors (29).

Quantification of Total 5-Methylcytosine by High Performance Capillary Electrophoresis (HPCE)—Quantification of the degree of methylation was carried out as previously described (30, 31). Briefly, genomic DNA (3–5 μg) was obtained by standard procedures and DNA hydrolysis was carried out with 1.25 μl (200 units/ml) of nuclease P1 for 16 h at 37 °C. Subsequently, alkaline phosphatase was added and mixtures were incubated for an additional 2 h at 37 °C. Hydrolyzed samples were injected under pressure (0.3 p.s.i.) for 3 s into an uncoated fused-silica capillary in a CE system (P/AC™ MDQ, Beckman-Coulter). Quantification of the relative methylation of each DNA sample was determined as the percentage of 5-methylcytosine (^{m}C) of total cytosines: ^{m}C peak area × 100/(C peak area + ^{m}C peak area). All samples were analyzed in duplicate, and three analytical measurements were made per replicate.

Quantification of Whole Histone H4 Acetylation and Methylation of Lysine 20 by HPCE—Quantification of acetylation and methylation at lysine 20 of histone H4 was done by a modification of the method

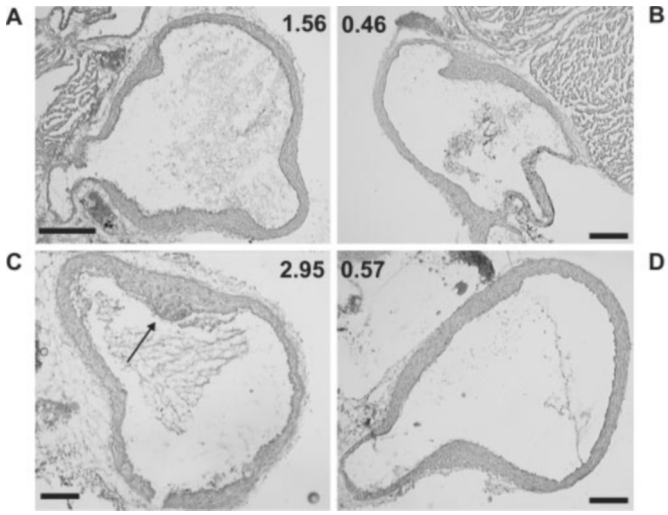

FIG. 1. **Atherosclerotic lesions in *Apoe*$^{-/-}$ mice at different ages.** Panels are cryosections of the ascending aorta of *Apoe*$^{-/-}$ (*A* and *C*) and WT (*B* and *D*) mice at the age of 4 weeks (*A* and *B*) and 6 months (*C* and *D*). The *arrow* in *C* indicates a fibrocellular lesion. *Numbers* in each photograph represent plasma total cholesterol levels (mg/ml). Staining, Oil Red O and hematoxylin. Original magnification, ×20. *Bar*, 0.2 mm.

previously described (32). Individual histone fractions were obtained from cell nuclei (33), and further purified by reversed-phase HPLC (34). The non-, mono-, di-, tri-, and tetra-acetylated forms of histones H3 and H4 and trimethylated H4 at lysine 20 were resolved by HPCE, using an uncoated fused-silica capillary (Beckman-Coulter™) (60.2 cm × 75 mm, effective length 50 cm) in a CE system (P/ACE™ MDQ, Beckman-Coulter™). The running buffer was 100 mM phosphate buffer, pH 2.0, containing 0.02% (w/v) HPM-cellulose. Running conditions were 25 °C and operating voltages of 12 kV. On-column absorbance was monitored at 214 nm. Before each run, the capillary system was conditioned by washing with 0.1 M NaOH for 3 min, and with 0.5 M H_2SO_4 for 2 min, and equilibrated with running buffer for 3 min. Buffers and washing solutions were prepared with Milli-Q water and filtered throughout 0.45-μm filters. Samples were injected under pressure (0.3 p.s.i.) for 3 s. All samples were analyzed in duplicate, and three analytical measurements were made per replicate.

Statistics—Comparisons were made by using nonparametric tests in the StatView (Abacus Concept, Berkeley, CA) or Statistica (StatSoft, Tulsa, OK) program for Macintosh. The counts of DNA methylation polymorphic bands were compared in samples paired by selective primer, using the Wilcoxon paired test. In all other cases, tests are specified under "Results."

RESULTS

Changes in PBMC and Aortic DNA Methylation Profiles Precede Fibrocellular Vascular Lesions in Apoe$^{-/-}$ *Mice*—To study DNA methylation patterns during the progression of atherosclerosis, 4-week-old and 6-month-old APOE-null (*Apoe*$^{-/-}$) were used. Mice were fed normal rodent diet, to exclude any confounding contribution of dietary factors potentially affecting DNA methylation (35). At the age of 4 weeks, mutant mice were hypercholesterolemic but lacked any detectable fatty streak or fibrocellular lesions at the ascending aorta or at the aortic arch (Fig. 1, *A* and *B*). By contrast, lesions consisting of a fibrocellular intima and a lipid-rich core were detectable in the same portion of the aortic vessel in 6-month-old *Apoe*$^{-/-}$ mice as previously reported (Fig. 1, *C* and *D*) (20). Plasma total cholesterol was markedly elevated in *Apoe*$^{-/-}$ mice of both age groups, relative to WT controls (Fig. 1, compare *A* and *C* with *B* and *D*) (20).

To screen PBMC for DNA methylation polymorphisms (DMPs) between *Apoe*$^{-/-}$ mice and matched controls, we exploited the MSAP fingerprinting technique. This technique is a modification of amplified fragment length polymorphism, a procedure that is based on random amplification of restriction fragments typically generated by digestion of genomic DNA with the EcoRI and MseI restriction enzymes (25). In MSAP, MseI is replaced by the methylation-sensitive enzyme HpaII, blocked by methylation at either cytosine residue in the recognition site 5′-CCGG-3′ (24). Following digestion of genomic DNA, adaptors are attached to restriction sites that have been successfully digested. It follows that the products of the MSAP ligation reaction consist of DNA fragments that are flanked by hypomethylated HpaII and EcoRI sites. Thereafter, two consecutive PCR reactions, a preamplification and a selective amplification, are performed to enrich a subpopulation of the restriction fragments. The primers employed are complementary to the core sequence of adaptors and recognition sites of the restriction enzymes, and the number of nucleotides added to their 3′ terminus determines their selectivity. Typically the number of selective nucleotides is increased in the selective amplification, where one of the two primers is radioactively labeled. This enables the visualization of a subset of restriction fragments by autoradiography following acrylamide gel electrophoresis.

PBMC DNA was screened by MSAP, using 23 different combinations of selective primers, corresponding to a total of ~1,600 bands/genotype group. Parallel MSAP analyses were conducted with MspI, an isoschizomer of HpaII that is only sensitive to methylation at the external cytosine (methylation at CNG trinucleotide) on one or both strands (methylation on one strand only is referred to as hemimethylation). It follows that an HpaII polymorphism between WT and *Apoe*$^{-/-}$ samples can be attributed to differential CG methylation, if the corresponding MspI profile is monomorphic, *i.e.* either present or absent in both genotypes (Fig. 2*A*). In the latter case, the HpaII site is hemimethylated at the external cytosine in both genotypes (*lower bands* in Fig. 2*A*) (36). Alternatively, absence of MspI fragments may result from inefficient amplification of the more complex MspI amplicons, relative to HpaII products. Nonetheless, the stability of MspI profiles observed throughout our study argues against this hypothesis. A polymorphism detected with both HpaII and MspI digestion is indicative of CNG methylation or mutation at the targeted *Apoe* alleles or elsewhere (Fig. 2*B*).

The analysis revealed that polymorphisms were present at both 4 weeks and 6 months of age (Fig. 3). Although DMPs may contain internal hypermethylated HpaII or EcoRI sites, previous analyses revealed that the vast majority of MSAP products represent HpaII-EcoRI fragments that lack any internal HpaII or EcoRI site (37). Accordingly, in the present study, only 5% of the sequenced MSAP fragments (see below) contained an internal HpaII site and none contained any EcoRI site. This implies that hypermethylation of internal fragment sites affects only marginally, if at all, the assessment of genome methylation status by MSAP band scoring. Two hundred and eight of the 206 polymorphisms observed at 4 weeks and 6 months (counting polymorphisms that are common to both ages only once) represented changes in CG methylation, *e.g.* genuine DMPs (Fig. 3, *A* and *B*), whereas only one band represented a difference in CNG methylation or a mutation (Fig. 3*C*).

The total number of DMPs in 4-week-old PBMC was 48, or 3.2% of total bands. A similar analysis conducted on 6-month-old mice revealed that the total number of DMPs was increased by 3.8-fold to 185, or 11% of total bands, compared with the younger age group ($p < 0.002$). DMPs that were present in both age groups represented a substantial part of all DMPs at 4 weeks (27 of 48, or 56%), but were a minority at 6 months (15%).

An identical MSAP analysis was conducted on aortic DNA, using 14 selective primer combinations, producing a total of ~1,000 bands. Aortic DMPs showed a markedly different dis-

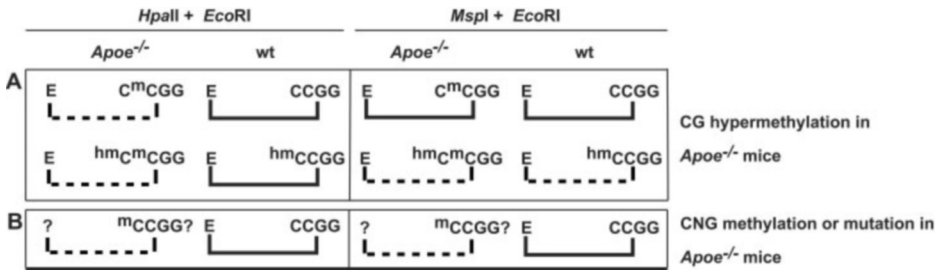

FIG. 2. **Outcome and interpretation of MSAP analysis.** Figure shows a schematic representation of banding patterns obtained by digestion of *Apoe*$^{-/-}$ or WT DNA with HpaII and EcoRI or MspI and EcoRI. *Solid* and *dashed lines* indicate present and absent bands, respectively. For clarity, only polymorphisms characterized by bands specifically present in WT DNA are shown. Flanking EcoRI (*E*) and HpaII/MspI (*CCGG*) sites are shown. The methylation status of the HpaII/MspI site is also indicated (^{hm}C, hemimethylated cytosine, *i.e.* methylated on one strand only). *Question marks* indicate possible presence of a mutation.

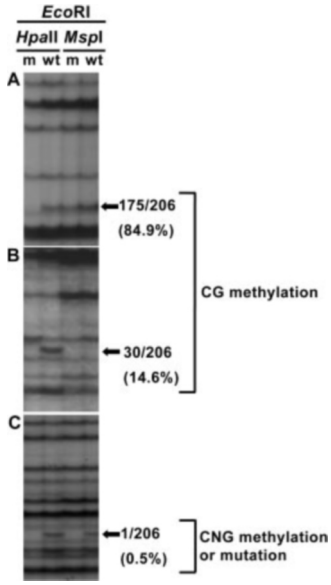

FIG. 3. **The majority of polymorphisms detected by MSAP in PBMC represent changes in CG methylation.** Representative examples of MSAP analysis of PBMC DNA of *Apoe*$^{-/-}$ mutant and WT mice (*m* and *WT*, respectively) digested with the indicated enzymes. The frequency and cause of polymorphisms are indicated on the *right*. *Figures* represent the number of bands of a given polymorphism/number of total PBMC polymorphisms (*i.e.* at 4 weeks and 6 months, counting polymorphisms common to both ages only once). *A*, DMP characterized by the presence of the MspI product in both genotypes. *B*, DMP characterized by the absence of any MspI product from both genotypes. *C*, polymorphism characterized by variability in both HpaII and MspI products.

tribution, in comparison with PBMC DNA. The total number of DMPs showed little or no increase with age, being 76 and 83 (or 7.6% and 8.3% of total bands) at 4 weeks and 6 months, respectively. Furthermore, approximately one third of DMPs were conserved in both age groups. The comparison of PBMC and aortic MSAP analyses revealed that few DMPs were common to the PBMC and the aorta (2 of 137 total aortic DMPs at 4 weeks and 6 months, counting polymorphisms that are common to both ages only once).

Further MSAP analysis was conducted on pericardial fat and liver of 6-month-old mice by using six primer combinations. In these tissues, the frequency of DMPs was severalfold lower than in matched PBMC and aorta (*i.e.* 0.5–1% of total bands; $p < 0.03$ in all comparisons). This indicates that the bulk of DMPs observed in *Apoe*$^{-/-}$ mice from the age of 4 weeks on represented genotype-related and tissue-specific, rather than reflecting inter- or intra-individual epigenetic variations that are unrelated to the *Apoe* genotype (see, for example, Ref. 38).

Hypo- and Hypermethylation in Apoe$^{-/-}$ *Mice*—A DMP that is characterized by a band specifically present in *Apoe*$^{-/-}$ mutant (MDMP) or WT (WDMP) mice, implies hypo- or hypermethylation at the flanking HpaII site, respectively, in *Apoe*$^{-/-}$ mice compared with WT. Previous comparisons of parallel results obtained with MSAP and direct quantitation of ^{m}C by HPCE, established that the total number of bands produced by MSAP accurately reflects the genome-wide methylation status of a particular DNA sample (37). Therefore, the relative proportion of MDMPs and WDMPs allows the estimation of the level of hypo- or hypermethylation of *Apoe*$^{-/-}$ DNA.

Both MDMPs and WDMPs were observed in all samples analyzed, albeit at a different relative extent in different tissues and age groups, indicating that hypo- and hypermethylation occurred simultaneously in *Apoe*$^{-/-}$ DNA (Table I). In 4-week-old mice, the relative proportion of MDMPs and WDMPs was similar in PBMC, whereas a significant excess of MDMPs was observed in the aorta (Table I). By contrast, MDMPs were significantly more frequent than WDMPs in both PBMC and aorta of 6-month-old mice (Table I). The net extent of *Apoe*$^{-/-}$ DNA hypomethylation, was measured by dividing the difference between the number of MDMPs and WDMPs by the total number of bands. DNA hypomethylation did not exceed ~4% and was higher in the aorta compared with PBMC (Table I).

To corroborate the result of the MSAP analysis, we assessed the relative methylation status of *Apoe*$^{-/-}$ and control DNA, by the *Sss*I methyl-accepting assay. *Sss*I methyltransferase is a bacterial enzyme that transfers methyl groups to cytosine residues in a CG dinucleotide context, using SAM as a methyl group donor. If labeled SAM is used in the reaction, the incorporation of radioactivity in DNA is proportional to the extent of initial hypomethylation. In accordance with the data obtained by MSAP, 4-week-old *Apoe*$^{-/-}$ aortic, but not PBMC DNA, showed a significant decline in global methylation, whereas hypomethylation was detected in both samples of older *Apoe*$^{-/-}$ mice (Fig. 4, *A* and *B*). By contrast, no significant difference in liver or skeletal muscle DNA methylation was detected between *Apoe*$^{-/-}$ and control mice (Fig. 4, *A* and *B*). Furthermore, the *Sss*I methyl-accepting assay allows to estimate the number of demethylated CG sites in *Apoe*$^{-/-}$ mice relative to controls, and therefore yields an estimation of the relative extent of global DNA hypomethylation. Again in accordance with the results of MSAP, DNA hypomethylation was more pronounced in the aorta, compared with PBMC (0.40×10^5 ($n = 5$) and 0.64×10^5 ($n = 12$) demethylated CG sites/haploid genome, respectively) at 6 months, and was lower than either sample in aortas of 4-week-old mice (0.25×10^5 ($n = 12$); compare with values in Table I).

Characterization of Variably Methylated Sequences—To characterize the PBMC DMPs, MSAP fragments were excised from acrylamide gels, reamplified by PCR, cloned, and subjected to sequencing in triplicate. The following DMPs were chosen: all the age-independent DMPs, all 4-week-specific DMPs, and 29 randomly chosen 6-month-specific DMPs. Sixty

TABLE I
Hypo- and hypermethylation in Apoe$^{-/-}$ mice

p values refer to differences in DMP counts (χ^2 test). NS, not significant ($p > 0.05$). NC, not calculated.

Type of DMP	PBMC		Aorta	
	4 weeks	6 months	4 weeks	6 months
MDMPs	26	111	45	62
WDMPs	22	74	31	21
p	NS	<0.04	<0.02	<0.003
Extent of net DNA hypomethylation (%)	NC	2.5	1.4	4.1

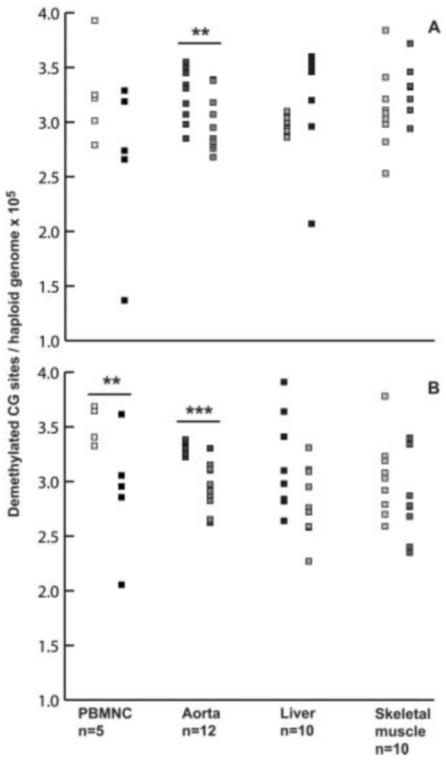

FIG. 4. **Genome hypomethylation is tissue-specific in *Apoe*$^{-/-}$ mice.** Figure is a SssI methyl-accepting assay showing the extent of incorporation of tritiated methyl groups into DNA from 4-week-old (*A*) and 6-month-old (*B*) mice. Each data point represents an individual mouse. The analyzed tissue and sample size are indicated at the *bottom* of the figure. For each tissue, data points relative to *Apoe*$^{-/-}$ and WT DNA are on the *left* and *right side*, respectively. Significantly different samples are indicated by *asterisks*.

fragments were successfully sequenced, ranging from 60 to 543 bp in size. Twenty-four PBMC DMPs matched data base sequences, all of which were murine (Table II). The majority of DMPs exhibited identity to relatively uncharacterized mouse genomic sequences. The remaining DMPs showed homology with repeated elements, as well as with ESTs (Table II). A reverse transcription-PCR-based expression analysis was conducted in 6-month-old mice for selected clones displaying homology to ESTs or genomic sequences (M1, M42, M45, M46, and M49; Table II). Two DMPs, one of which homologous to an EST (M45 and M49) showed specific expression in *Apoe*$^{-/-}$ PBMC (data not shown), in accordance with their hypomethylated status in that group.

Based on the above data, we could not estimate the relative contribution of genic sequences and interspersed repeated elements to the observed changes of DNA methylation patterns in *Apoe*$^{-/-}$ mice. To clarify this issue, we analyzed the methylation status of the highly repeated LINE-1 retrotransposon elements in aortic DNA by Southern blotting. In tumors, demethylation of LINE-1 sequences, detected by the appearance of

TABLE II
PBMC DMP sequences with significant matches in data bases

Lowest *E* value of data base matches was 10^{-58}. SINE, short interspersed nuclear element; LTR, long terminal repeat; ERVK, endogenous retrovirus K.

Clone	Size	Accession no.	Type of sequence
	bp		
M1	152	BM875787	EST
M4	253	AC132863	SINE
M7	167	AC115816	Genomic
M12	131	AC024607	Genomic
M26	301		LTR/ERVK
M27	303	AC102506	Genomic
M30	216	BX322546	Genomic
M42	157	AL807763	Genomic
M45	107	AC135019	Genomic
M46	285	AC122350	Genomic
M49	141	BY249272	EST
M50	61	AC140236	Genomic
M52	223	AC103622	Genomic
M54	383	AC120437	Genomic
M55	226	AC101290	Genomic
M58	236		LINE
M62	295		LTR
sz44	317	AC103664	Genomic
sz47	181		LINE
sz23	89	AC129780	Genomic
szc7	543		SINE
szc9	458	AC101947	Genomic
szc13	340	AC115970	Genomic
szc14	343		LINE

bands in the 1–4-kb range after digestion with HpaII, is a landmark of global genomic hypomethylation (39). However, no obvious hypomethylation of LINE-1 sequences was detected in the aortic tissue of 6-month-old *Apoe*$^{-/-}$ mice (data not shown).

Southern Blotting and HpaII-sensitive PCR Analysis of DMPs—DMP profiles and their tissue specificity were verified by Southern blotting and HpaII-sensitive PCR of seven randomly chosen PBMC DMPs. Representative results of four DMPs are shown in Fig. 5. The WDMP M27 is a 304-bp MSAP fragment that was hypermethylated in both 4-week-old and 6-month-old *Apoe*$^{-/-}$ mice. Accordingly, Southern blotting analysis revealed that the M27 probe hybridized to a band of approximately the expected size in WT PBMC DNA digested with HpaII and EcoRI, and in all samples digested with MspI and EcoRI (Fig. 5*A*, *arrow*), whereas it hybridized to higher size fragments in *Apoe*$^{-/-}$ DNA from both age groups. By contrast, hybridization of M27 to liver DNA-digested HpaII and EcoRI did not reveal any polymorphism (Fig. 5*A*). In HpaII-sensitive PCR, genomic DNA digested with HpaII was amplified with a primer internal to the DMP fragment, and an external primer, deduced by data base match sequences. Because primers were placed at opposite sides of the DMP-flanking HpaII site, a product could be obtained only if the corresponding HpaII site was methylated. *Apoe*$^{-/-}$ tail DNA was used as control to assess the tissue specificity of DNA methylation patterns. The analysis showed that the amplification of MDMPs M4 and M54 was reduced in 4-week-old *Apoe*$^{-/-}$ PBMC, relative to matched WT PBMC or tail DNA, in accordance with their hypomethylated status in *Apoe*$^{-/-}$ PBMC (Fig. 5*B*). The opposite pattern was produced by the WDMP sz44, as expected (Fig. 5*B*). Amplification following MspI digestion failed to yield any product in all cases (data not shown).

Effects of Lipoproteins on DNA Methylation and Histone H4 Modifications in THP-1 Cells—The occurrence of both local hyper- and hypomethylation of *Apoe*$^{-/-}$ DNA at the initial stages of atherosclerosis suggests that at least a subset of the observed changes in DNA methylation profiles are active cellular responses to proatherogenic factors. The latter may in-

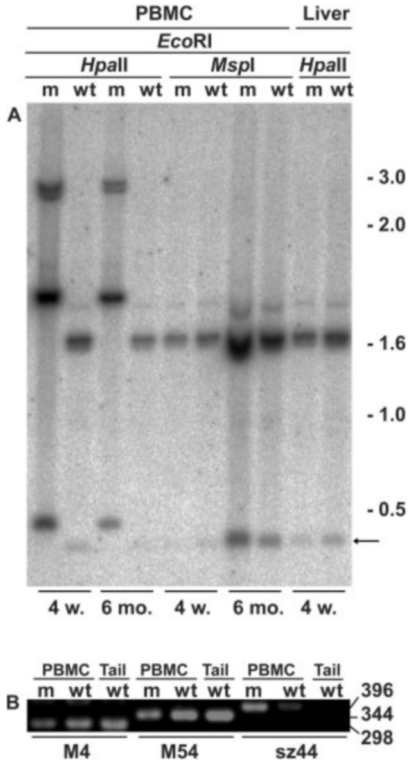

FIG. 5. **Analysis of DMPs by Southern blotting and HpaII-sensitive PCR.** *A*, Southern blot analysis conducted with a probe corresponding to PBMC DMP M27. The *arrow* indicates the position of genomic hybridizing fragment corresponding to the MSAP DMP. Size of DNA markers are shown on the *right* (kb). *B*, HpaII-sensitive PCR analysis of the indicated PBMC DMPs at 4 weeks. Expected sizes of PCR products were 282, 327 and 399 bp, respectively. Size of DNA markers is shown on the *right* of gel (bp). Abbreviations are as in the legend of Fig. 3.

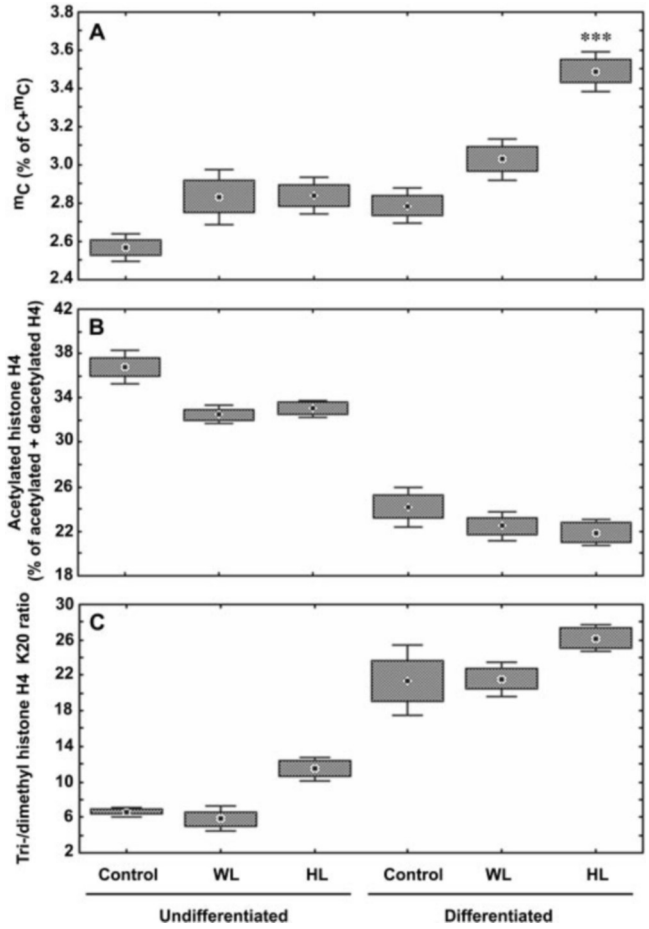

FIG. 6. **Effects of lipoproteins on DNA methylation and histone H4 post-translational modifications in THP-1 cells.** Panels show box and Whisker plots of the effects of the WL and HL lipoprotein mixtures on ^{m}C content (*A*), levels of acetylated histone H4 (*B*), and ratio between tri-methylated and di-methylated histone H4 lysine 20 (*C*) in undifferentiated and differentiated THP-1 cells. *Control*, incubation without lipoproteins. *HL* and *WL*, high and low VLDL+LDL lipid mixtures, respectively, as described under "Results." The average of triplicate measurements, with S.D. and S.E., are shown for each sample. *Asterisks* represent the significance levels compared with matched controls (Scheffe test).

clude deranged levels of lipoproteins, because hyperlipidemia plays a pivotal role in the initiation of atherosclerosis and precedes the appearance of vascular lesions in *Apoe*$^{-/-}$ mice. To verify this hypothesis, we stimulated the human monocytic THP-1 cells with a mixture of VLDL, LDL, and HDL, and explored the effects on global genomic DNA methylation, by measuring the relative content of ^{m}C. THP-1 cells can differentiate into macrophage-like cells by treatment with phorbol esters, and are therefore a model for studying the role of inflammatory cells in atherosclerosis (21). Two lipoprotein mixtures were used. The first contains lipoproteins at relative plasma proportions consistently observed during our previous studies of *Apoe*$^{-/-}$ mice (68.8 μg/ml VLDL, 32.1 μg/ml LDL, 91.1 μg/ml HDL, referred to as HL mixture). The second mixture reproduces relative lipoprotein proportion of WT mice (4.3 μg/ml VLDL, 2.9 μg/ml LDL, 116 μg/ml HDL, referred to as WL mixture). The HL and WL mixture differ for the ratio between the composite amount of the atherogenic VLDL and LDL particles, and the amount of the antiatherogenic HDL (1.11 and 0.06, respectively), corresponding to an 18-fold higher ratio in the HL, relative to the WL mixture. In absolute terms, the HL and WL mixtures contained one tenth of the lipoprotein concentrations present in their *in vivo* counterpart, or a maximum cumulative concentration of 100.9 μg/ml VLDL + LDL. These concentrations were chosen as too high lipoprotein levels are cytotoxic, and incubation with up to 150 μg/ml VLDL for 24 h do not induce cell death in THP-1 cells (data not shown).

Stimulation of differentiated THP-1 cells with HL mixture for 24 h induced a significant increase in DNA methylation, compared with matched controls or cells stimulated with the WL mixture ($p < 0.0003$, Scheffe test), whereas the latter treatment had no significant effect (Fig. 6*A*). By contrast, no statistically significant effect of lipoproteins was observed in undifferentiated THP-1 cells (Fig. 6*A*). To further understand the effects of lipoproteins on chromatin structure, we analyzed two post-translational modifications of the histone H4, namely acetylation and methylation at lysine 20 (Lys-20). H4 acetylation is generally associated with a transcriptionally active state, whereas deacetylation is associated with gene silencing and heterochromatin formation (40). Furthermore, trimethylation of Lys-20 of H4 has been associated with silent chromatin and aging (41, 42). Increasing doses of VLDL and LDL had no statistically significant effect on either histone modification (Kruskal-Wallis analysis of variance), whereas differentiated cells showed a significant decrease in histone H4 acetylation and an increase in H4 tri-/dimethyl-Lys-20 ratio, both landmarks of heterochromatin formation ($p < 0.0003$ for both, Scheffe test, Fig. 6, *B* and *C*). Overall, the triple global pattern of hypermethylation of DNA and H4, and loss of histone acetylation observed in the cells treated with atherogenic lipoproteins, suggest that gene silencing and the formation of heterochromatin are early molecular "hits" that precede, and probably contribute to, the histopathological traits associated with atherosclerosis.

DISCUSSION

The present work expands the current knowledge on the role of DNA methylation in atherosclerosis, by showing that DMPs are present prior to the appearance of vascular lesions in *Apoe*$^{-/-}$ mice. Noticeably, DMPs were significantly more frequent in organs and cell types involved in the initiation and progression of atherosclerosis, *e.g.* the aorta, circulating inflammatory cells, and/or immune cells (43, 44), in comparison with the control tissues examined (liver, pericardial fat, skeletal muscle). Furthermore, few DMPs were common to PBMC and the aorta, mirroring the functional differences between the two tissues. Taken together, the observed mosaicism and tissue specificity of DMPs suggest that these epigenetic marks are specifically associated with predisposition to and progression of atherosclerosis, rather than originating from genetic or stochastic epigenetic variability. An additional factor known to affect DNA methylation patterns is transgene integration, implying that a similar effect may be exerted by the insertion of exogenous sequences into targeted *Apoe* alleles (45). Nevertheless, the mosaic nature of the observed DMP strongly argues against such a mechanism.

In agreement with previous studies, we observe a modest, but significant global hypomethylation of genomic DNA in aortas and PBMC of *Apoe*$^{-/-}$ mice afflicted by fibrocellular lesions (18, 19). The extent of aortic DNA hypomethylation observed in our study was lower in comparison with the corresponding value obtained by Hiltunen and colleagues (18) in *Apoe*$^{-/-}$ mice, humans, and rabbits. These discrepancies have several possible explanations. First, Hiltunen and colleagues assessed the effects of dietary lipids, regardless of the consequences of atherosclerosis *per se* in *Apoe*$^{-/-}$ mice (*e.g.* in comparison with matched WT mice). Similarly, the work conducted by the same group in rabbits analyzed the epigenetic effects of dietary lipids and cell proliferation following arterial denudation, rather than genuine atherosclerosis. Furthermore, the measurement of DNA methylation in human atherosclerotic lesions is potentially affected by inter- and even intra-individual epigenetic variability, particularly in samples that are forcibly of relatively limited size (18, 38). In accordance with the modest net DNA hypomethylation estimated by MSAP, methylation of LINE-1 sequences was not detectably changed in *Apoe*$^{-/-}$ aortic DNA compared with controls. Taken together, these observations suggest that the mechanism of genome hypomethylation differs in atherosclerosis, cancer, and aging, and that similarities between the epigenetics of these pathophysiological situations must be drawn with caution. Our results suggest that atherosclerosis is associated with a significant rearrangement of DNA methylation patterns, including both hyper- and hypomethylation, in the PBMC and the aorta. The samples analyzed in this study represent heterogeneous cell populations; therefore, more extreme changes in DNA methylation, perhaps including hypomethylation to levels observed in cancer and aging, cannot be excluded to occur in selected cell types. The results of sequencing and expression analysis suggest that at least some of the observed DMPs represent genic sequences.

Correlative studies suggest that DNA hypomethylation may be a passive phenomenon because of the depletion of cellular SAM in hyperhomocysteinemia (19, 46, 47). However, hyperhomocysteinemia is not a trait of *Apoe*$^{-/-}$ mice, implying that the process is not merely a passive consequence of the depletion of cellular SAM (48). Rather, our results suggest that DMPs are the compound result of active and passive mechanisms. The finding that lipoproteins induce DNA hypermethylation in cultured cells suggests that changes in DNA methylation are among the earliest cellular changes in atherosclerosis. Furthermore, these observations demonstrate for the first time a direct link between a pro-atherogenic factor (the hyperlipidemic lipoprotein profile) and changes in DNA methylation. Our results are consistent with the observation that the atheroprotective HDL causes chromatin activation in cell culture (49). As the disease progresses, and the involvement of SMC becomes more significant (43), hyperproliferation of the latter cell type in the fibromuscular lesion may then tip the balance of global genome methylation status toward hypomethylation, as previously shown (18). The mechanisms by which lipoproteins can affect DNA methylation patterns are currently not understood. APOA-I, a constituent of HDL, is physically associated with active chromatin and binds to a CG-rich oligonucleotide *in vitro*, suggesting a role for lipoprotein constituents in chromatin binding and remodeling (50, 51). Further studies are necessary to elucidate the functional consequences of these interactions in atherogenesis.

Incidentally, we show that deacetylation and increased trimethylation of histone H4 lysine 20 occur in differentiated, unstimulated THP-1 cells in the absence of a significant DNA hypermethylation. Further investigations are needed to interpret this result in the light of the current models of heterochromatin formation (52, 53).

In conclusion, we report that specific changes in DNA methylation occur during the early phases of atherosclerosis in a mouse model. Furthermore, by showing that DMPs are present in accessible cell types such as PBMC at early stages of atherosclerosis, our work points to epigenetic marks as potential novel tools for prevention and therapy.

Acknowledgments—We thank Finn Cilius Nielsen for support and for critically reading the manuscript, Pernille Ekstrøm and Birgitte Petersen for excellent technical and secretarial help, and members of the laboratories in Malmø and Copenhagen for discussion and encouragement.

REFERENCES

1. Ross, R. (1999) *N. Engl. J. Med.* **340,** 115–126
2. Jeltsch, A. (2002) *Chem. Bio. Chem.* **3,** 274–293
3. Chen, R. Z., Pettersson, U., Beard, C., Jackson-Grusby, L., and Jaenisch, R. (1998) *Nature* **395,** 89–93
4. Li, E. (2002) *Nat. Rev. Genet.* **3,** 662–673
5. Jaenisch, R., and Bird, A. (2003) *Nat. Genet.* **33,** 245–254
6. Hashimshony, T., Zhang, J., Keshet, I., Bustin, M., and Cedar, H. (2003) *Nat. Genet.* **34,** 187–192
7. Issa, J.-P. (2002) *J. Nutr.* **132,** 2388S–2392S
8. Feinberg, A. P., and Tycko, B. (2004) *Nat. Rev. Cancer* **4,** 143–153
9. Esteller, M., and Herman, J. G. (2002) *J. Pathol.* **196,** 1–7
10. Laird, P. W. (2003) *Nat. Rev. Cancer* **3,** 253–266
11. Newman, P. E. (1999) *Med. Hypotheses* **53,** 421–424
12. Dong, C., Yoon, W., and Goldschmidt-Clermont, P. J. (2002) *J. Nutr.* **132,** 2406S–2409S
13. Hiltunen, M. O., and Ylä-Herttuala, S. (2003) *Arterioscler. Thromb. Vasc. Biol.* **23,** 1750–1753
14. Issa, J.-P. (1999) *Crit. Rev. Oncol. Hematol.* **32,** 31–43
15. Brattström, L., and Wilcken, D. E. L. (2000) *Am. J. Clin. Nutr.* **72,** 315–323
16. Chen, Z., Karaplis, A. C., Ackerman, S. L., Pogribny, I. P., Melnyk, S., Lussier-Cacan, S., Chen, M. F., Pai, A., John, S. W. M., Smith, R. S., Bottiglieri, T., Bagley, P., Selhub, J., Rudnicki, M. A., James, S. J., and Rozen, R. (2001) *Hum. Mol. Gen.* **10,** 433–443
17. Laukkanen, M. O., Mannermaa, S., Hiltunen, M. O., Aittomäki, S., Airenne, K., Jänne, J., and Ylä-Herttuala, S. (1999) *Arterioscler. Thromb. Vasc. Biol.* **19,** 2171–2178
18. Hiltunen, M. O., Turunen, M. P., Hakkinen, T. P., Rutanen, J., Hedman, M., Makinen, K., Turunen, A. M., Aalto-Setala, K., and Ylä-Herttuala, S. (2002) *Vasc. Med.* **7,** 5–11
19. Castro, R., Rivera, I., Struys, E. A., Jansen, E. E. W., Ravasco, P., Camilo, M. E., Blom, H. J., Jakobs, C., and Tavares de Almeida, I. (2003) *Clin. Chem.* **49,** 1292–1296
20. Zhang, S. H., Reddick, R. L., Piedrahita, J. A., and Maeda, N. (1992) *Science* **258,** 468–471
21. Auverx, J. (1991) *Experientia* (*Basel*) **47,** 22–31
22. Popesko, P., Rajtova, V., and Horak, J. (1992) *A Colour Atlas of Anatomy of Small Laboratory Animals*, Vol. 2, pp. 105–166, Wolfe Publishing, London, United Kingdom
23. Zaina, S., Pettersson, L., Ahrén, B., Brånén, L., Hassan, A. B., Lindholm, M., Mattsson, R., Thyberg, J., and Nilsson, J. (2002) *J. Biol. Chem.* **277,** 4505–4511
24. Reina-Lopez, G. E., Simpson, J., and Ruiz-Herrera, J. (1997) *Mol. Gen. Genet.* **253,** 703–710
25. Vos, P., Hogers, R., Bleeker, M., Reijans, M., van de Lee, T., Hornes, M., Frijters, A., Pot, J., Peleman, J., Kuiper, M., and Zabeau, M. (1995) *Nucleic*

Acids Res. **23,** 4407–4414
26. Schmitt, F., Oakeley, E. J., and Jost, J. P. (1997) *J. Biol. Chem.* **272,** 1534–1540
27. Santourlidis, S., Florl, A., Ackermann, R., Wirtz, H.-C., and Schulz, W. A. (1999) *The Prostate* **39,** 166–174
28. Furano, A. V. (2000) *Prog. Nucleic Acids Res. Mol. Biol.* **64,** 255–294
29. Lindholm, M., Sjoblom, L., Nordborg, C., Ostlund-Lindqvist, A. M., and Eklund, A. (1993) *Ann. Nutr. Metab.* **37,** 302–310
30. Fraga, M. F., Uriol, E., Borja Diego, L., Berdasco, M., Esteller, M., Canal, M. J., and Rodríguez, R. (2002) *Electrophoresis* **23,** 1677–1681
31. Ballestar, E., Paz, M. F., Valle, L., Wei, S., Fraga, M. F., Espada, J., Cigudosa, J. C., Huang, T. H., and Esteller, M. (2003) *EMBO J.* **22,** 6335–6345
32. Lindner, H., Helliger, W., Dirschlmayer, A., Talasz, H., Wurm, M., Sarg, B., Jaquemar, M., and Puschendorf, B. (1992) *J. Chromatogr.* **608,** 211–216
33. Goodwin, G. H., Nicolas, R. H., and Johns, E. W. (1977) *Biochem. J.* **167,** 485–488
34. Gurley, L. R., Prentice, D. A., Valdez, J. G., and Spall, W. D. (1983) *Anal. Biochem.* **131,** 465–477
35. Friso, S., and Choi, S.-W. (2002) *J. Nutr.* **132,** 2382S-2387S
36. McClelland, M., Nelson, M., and Raschke, E. (1994) *Nucleic Acids Res.* **22,** 3640–3659
37. Lauria, M., Rupe, M., Guo, M., Kranz, E., Pirona, R., Viotti, A., and Lund, G. (2004) *Plant Cell* **16,** 510–522
38. Yatabe, Y., Tavaré, S., and Shibata, D. (2001) *Proc. Natl. Acad. Sci. U. S. A.* **98,** 10839–10844
39. Schulz, W. A., Elo, J. P., Florl, A. R., Pennanen, S., Santourlidis, S., Engers, R., Buchardt, M., Seifert, H. H., and Visakorpi, T. (2002) *Genes Chromosomes Cancer* **35,** 58–65
40. Richards, E. J., and Elgin, S. C. (2002) *Cell* **108,** 489–500
41. Nishioka, K., Rice, J. C., Sarma, K., Erdjument-Bromage, H., Werner, J., Wang, Y., Chuikov, S., Valenzuela, P., Tempst, P., Steward, R., Lis, J. T., Allis, C. D., and Reinberg, D. (2002) *Mol. Cell.* **9,** 1201–1213
42. Sarg, B., Koutzamani, E., Helliger, W., Rundquist, I., and Lindner, H. H. (2002) *J. Biol. Chem.* **277,** 39195–39201
43. Steinberg, D. (2002) *Nat. Med.* **8,** 1211–1217
44. Hansson, G. K., Libby, P., Schönbeck, U., and Yan, Z.-Q. (2002) *Circ. Res.* **91,** 281–291
45. Müller, K., Heller, H., and Doerfler, W. (2001) *J. Biol. Chem.* **276,** 14271–14278
46. Yi, P., Melnyk, S., Pogribna, M., Pogribny, I. P., Hine, R. J., and James, S. J. (2000) *J. Biol. Chem.* **275,** 29318–29323
47. Ingrosso, D., Cimmino, A., Perna, A. F., Masella, L., De Santo, N. G., De Bonis, M. L., Vacca, M., D'Esposito, M., D'Urso, M., Galletti, P., and Zappia, V. (2003) *Lancet* **361,** 1693–1699
48. Moghadasian, M. H., McManus, B. M., Nguyen, L. B., Shefer, S., Nadji, M., Godin, D. V., Green, T. J., Hill, J., Yang, Y., Scudamore, C. H., and Frohlich, J. J. (2001) *FASEB J.* **15,** 2623–2630
49. Panin, L. E., Svechnikova, I. G., and Maianskaia, N. N. (1995) *Ukr. Biokhim. Zh.* **67,** 64–70
50. Panin, L. E., Polyakov, L. M., Kolosova, N. G., Russkikh, G. S., and Poteryaeva, O. N. (1998) *Membr. Cell Biol.* **11,** 631–640
51. Panin, L. E., Tuzikov, F. V., and Gimautdinova, O. I. (2003) *J. Ster. Biochem. Mol. Biol.* **87,** 309–318
52. Bird, A. (2002) *Genes Dev.* **16,** 6–21
53. Mutskov, V., and Felsenfeld, G. (2004) *EMBO J.* **23,** 138–149